The magnetohydrodynamic stagnation point flow of a nanofluid over a stretching/shrinking sheet with suction

Syahira Mansur[1], Anuar Ishak[2*], Ioan Pop[3]

[1]Department of Mathematics and Statistics, Faculty of Science, Technology and Human Development, Universiti Tun Hussein Onn Malaysia, 86400 Parit Raja, Batu Pahat, Johor, Malaysia

[2]School of Mathematical Sciences, Faculty of Science and Technology, Universiti Kebangsaan Malaysia, 43600 UKM Bangi, Selangor, Malaysia

[3]Department of Mathematics, Babeș-Bolyai University, 400084 Cluj-Napoca, Romania

*Corresponding author.
E-mail: anuar_mi@ukm.edu.my (A Ishak)
Tel.: +603 8921 5785; Fax: +603 8925 4519

Abstract

The magnetohydrodynamic (MHD) stagnation point flow of a nanofluid over a permeable stretching/shrinking sheet is studied. Numerical results are obtained using boundary value problem solver bvp4c in MATLAB for several values of parameters. The numerical results show that dual solutions exist for the shrinking case, while for the stretching case, the solution is unique. A stability analysis is performed to determine the stability of the dual solutions. For the stable solution, the skin friction is higher in the presence of magnetic field and increases when the suction effect is increased. It is also found that increasing the Brownian motion parameter and the thermophoresis parameter reduces the heat transfer rate at the surface.

Keywords: Boundary layer, heat transfer, magnetohydrodynamic, nanofluid, shrinking sheet, fluid mechanics

Introduction

Nanofluid refers to dispersion of nanoparticles in the base fluid. The inclusion of nanoparticles enhances thermal conductivity as reported by Masuda et al. [1]. Choi and

Eastman [2] discovered that the addition of less than 1% of nanoparticles doubles the heat conductivity of the base fluid. Two models have been constantly used by researchers to study the behaviour of nanofluids, namely the Tiwari-Das model [3] and Buongiorno model [4]. While Tiwari-Das model highlights the volumetric fraction of nanoparticles, Buongiorno model focuses on Brownian motion and thermophoresis effects. Buongiorno model was used in many recent papers, e.g. Nield and Kuznetsov [5-7], Kuznetsov and Nield [8, 9], Khan and Pop [10], Bachok et al. [11, 12], and Khan and Aziz [13], among others.

The boundary layer flow over a stretching sheet is significant in applications such as extrusion, wire drawing, metal spinning, hot rolling etc. [14]. Wang [15, 16], Mandal and Mukhopadhyay [17], Gupta and Gupta [18], Andersson [19], Ishak et al. [20] and Makinde and Aziz [21] are among various names whose papers on stretching sheet are published. However, to complement the study of stretching sheet, Miklavčič and Wang [22] then began the study of flow over a shrinking sheet in which they observed that the vorticity is not confined within a boundary layer and a steady flow cannot exist without exerting adequate suction at the boundary. However, Wang [23] reported that a stagnation flow may also be considered so that the velocity of the shrinking sheet is confined in the boundary layer. As the studies of shrinking sheet garner considerable attention, these findings prove to be crucial to these researches. Numerous studies on these problems have been conducted by researchers such as Fang et al. [24], Bachok et al. [25], Bhattacharyya et al. [26], Lok et al. [27,28], Zaimi et al. [29] and Roşca and Pop [30] among others.

Motivated by the above-mentioned researches, this paper aims at studying the magnetohydrodynamic (MHD) stagnation point flow of a nanofluid over a stretching/shrinking sheet with suction effect at the boundary which is the extension of a paper done by Ibrahim et al. [31]. MHD is the study of the dynamics of electrically conducting fluids such as plasmas, liquid metals and electrolytes The dependency of the skin friction coefficient and the local Nusselt number on five parameters, namely the stretching/shrinking, magnetic, velocity ratio, Brownian motion and thermophoresis parameters is the main focus of the present investigation. Numerical solutions are presented graphically and in tabular forms to show the effects of these parameters on the skin friction coefficient and the local Nusselt number.

Mathematical Formulation

We examine the boundary layer flow of a nanofluid towards a stagnation point on a permeable stretching/shrinking surface, kept at a constant temperature T_w and concentration C_w, at $y = 0$ as shown in Fig. 1, where the $x-$ and $y-$axes are taken along and normal to the stretching/shrinking surface. It is assumed that the free stream velocity is $U_\infty(x) = bx$ and the plate is stretched/shrunk with the velocity $u_w(x) = c\,x$ where b and c are positive constants. It is also assumed that the constant mass flux velocity is v_0 with $v_0 < 0$ for suction and $v_0 > 0$ for injection. The ambient values of the temperature and nanoparticle fraction are taken as T_∞ and C_∞, respectively. In view of thermal equilibrium, there is no slip between the base (or ordinary) fluid and suspended nanoparticles. Furthermore, the flow is subjected to a constant transverse magnetic field of strength $B = B_0$ which is assumed to be applied to the positive y-direction. Under these assumptions, the unsteady governing continuity, momentum and energy boundary layer equations are [31]

$$\frac{\partial u}{\partial x} + \frac{\partial v}{\partial y} = 0 \tag{1}$$

$$\frac{\partial u}{\partial t} + u\,\frac{\partial u}{\partial x} + v\frac{\partial u}{\partial y} = U_\infty \frac{dU_\infty}{dx} + \nu\frac{\partial^2 u}{\partial y^2} + \frac{\sigma B_0^2}{\rho_f}\left(U_\infty - u\right) \tag{2}$$

$$\frac{\partial T}{\partial t} + u\,\frac{\partial T}{\partial x} + v\frac{\partial T}{\partial y} = \alpha\frac{\partial^2 T}{\partial y^2} + \sigma\left[D_B\frac{\partial C}{\partial y}\frac{\partial T}{\partial y} + \frac{D_T}{T_\infty}\left(\frac{\partial T}{\partial y}\right)^2\right] \tag{3}$$

$$\frac{\partial C}{\partial t} + u\,\frac{\partial C}{\partial x} + v\frac{\partial C}{\partial y} = D_B\frac{\partial^2 C}{\partial y^2} + \frac{D_T}{T_\infty}\frac{\partial^2 T}{\partial y^2} \tag{4}$$

where u and v are the velocity components along the x- and y-axis respectively, U_∞ is the free stream velocity, t is time, T is the fluid temperature, α is the thermal diffusivity, ν is the kinematic viscosity, D_B is the Brownian diffusion coefficient, D_T is the thermophoresis diffusion coefficient and C is the nanoparticle volume fraction. Furthermore, $\sigma = (\rho c)_p / (\rho c)_f$ is the ratio between the effective heat capacity of the fluid with ρ_f and ρ_p being the density of the fluid and the density of the particles respectively and c_f and c_p denote the specific heat of the fluid and the particle at constant pressure, respectively.

The equations are subjected to the boundary conditions

$$
\begin{aligned}
&t<0: \quad u=v=0, \quad T=T_\infty, \quad C=C_\infty \quad \text{for any} \quad x, y \\
&t\geq 0: \quad v=v_0, \quad u=\lambda u_w(x), \quad T=T_w, \quad C=C_w \quad \text{at} \quad y=0 \\
&\qquad\quad u\to U_\infty(x), \quad T\to T_\infty, \quad C\to C_\infty \quad \text{as} \quad y\to\infty
\end{aligned} \tag{5}
$$

where λ is the stretching parameter with $\lambda > 0$ for stretching and $\lambda < 0$ for shrinking, and the subscript w denotes the values at the solid surface.

Steady-state flow

In order to solve the steady-state flow ($\partial/\partial t = 0$) of Eqs. (1) to (4) with the boundary conditions (5), we introduce the following similarity variable

$$
\begin{aligned}
&\psi=\sqrt{c\nu}\, x\, f(\eta), \quad \theta(\eta)=(T-T_\infty)/(T_f-T_\infty) \\
&\phi(\eta)=(C-C_w)/(C_w-C_\infty), \quad \eta=\sqrt{c/\nu}\, y
\end{aligned} \tag{6}
$$

where ψ is the stream function, which is defined as $u=\partial\psi/\partial y$ and $v=-\partial\psi/\partial x$. Thus, we have

$$
u=c\,x\,f'(\eta), \quad v=-\sqrt{c\nu}\, f(\eta) \tag{7}
$$

where prime denotes differentiation with respect to η.

Substituting variables (5) into Eqs. (2) and (3) for the steady-state flow ($\partial/\partial t = 0$), we obtain the following ordinary differential (similarity) equations

$$
f'''+f\,f''-f'^2+M\left(A-f'^2\right)+A^2=0 \tag{8}
$$

$$
\frac{1}{\mathrm{Pr}}\theta''+f\,\theta'+Nb\,\phi'\theta'+Nt\,\theta'^2=0 \tag{9}
$$

$$
\phi''+Le\,f\,\phi'+\frac{Nt}{Nb}\theta''=0 \tag{10}
$$

subject to the boundary conditions (4), which become

$$
\begin{aligned}
&f(0)=S, \quad f'(0)=\lambda, \quad \theta(0)=1, \quad \phi(0)=1 \\
&f'(\eta)\to A, \quad \theta(\eta)\to 0, \quad \phi(\eta)\to 0 \quad \text{as} \quad \eta\to\infty
\end{aligned} \tag{11}
$$

where Pr is the Prandtl number, M is the magnetic parameter, S is the constant mass transfer parameter with $S > 0$ for suction and $S < 0$ for injection, A is the velocity ratio, Le is the Lewis number, Nb is the Brownian motion parameter and Nt is the thermophoresis parameter, which are defined as

$$\Pr = \frac{\nu}{\alpha}, \quad Nb = \frac{\sigma D_B (\phi_w - \phi_\infty)}{\nu}, \quad Nt = \frac{\sigma D_T (T_w - T_\infty)}{\nu T_\infty}, \quad Le = \frac{\nu}{D_B},$$
$$S = -\frac{v_0}{\sqrt{a\nu}}, \quad M = \frac{\sigma B_0^2}{\rho_f c}, \quad A = \frac{b}{c} \tag{12}$$

The quantities of physical interest are the skin friction or shear stress coefficient C_f, and the local Nusselt number Nu_x, which are defined as

$$C_f = \frac{\tau_w}{\rho u_w^2(x)}, \quad Nu_x = \frac{x\, q_w}{k(T_f - T_\infty)} \tag{13}$$

where τ_w is the skin friction or shear stress along the plate and q_w is the heat flux from the plate, which are defined as

$$\tau_w = \mu \left(\frac{\partial u}{\partial y} \right)_{y=0}, \quad q_w = -k \left(\frac{\partial T}{\partial y} \right)_{y=0} \tag{14}$$

Using (5), (10) and (11), we get

$$\mathrm{Re}_x^{1/2} C_f = f''(0), \quad \mathrm{Re}_x^{-1/2} Nu_x = -\theta'(0) \tag{15}$$

where $\mathrm{Re}_x = u_w(x)\, x / \nu$ is the local Reynolds number.

Flow stability

It has been shown in some papers (Weidman et al. [32], Roşca and Pop [30], etc.) that dual (lower and upper branch) solutions exist. In order to determine which of these solutions are stable and physically realizable, a stability analysis to the solutions of Eqs. (1)-(5) needs to done. Following Weidman et al. [32], a dimensionless time variable τ is introduced. The use of τ is associated with an initial value problem and this is consistent with the question of which solution will be obtained in practice (physically realizable). Thus, the new variables for the unsteady problem are

$$\psi = \sqrt{c\nu}\, x\, f(\eta, \tau), \quad u = c\, x \frac{\partial f}{\partial \eta}(\eta, \tau), \quad v = -\sqrt{c\nu}\, f(\eta, \tau)$$
$$\theta(\eta, \tau) = (T - T_\infty)/(T_f - T_\infty), \quad \phi(\eta, \tau) = (C - C_\infty)/(C_w - C_\infty) \tag{16}$$
$$\tau = a\, t, \quad \eta = \sqrt{c/\nu}\, y$$

so that Eqs. (2) - (4) can be written as

$$\frac{\partial^3 f}{\partial \eta^3}+f\frac{\partial^2 f}{\partial \eta^2}-\left(\frac{\partial f}{\partial \eta}\right)^2+M\left(A-\frac{\partial f}{\partial \eta}\right)+A^2-\frac{\partial^2 f}{\partial \eta\,\partial \tau}=0 \tag{17}$$

$$\frac{1}{\Pr}\frac{\partial^2 \theta}{\partial \eta^2}+f\frac{\partial \theta}{\partial \eta}+Nb\frac{\partial \phi}{\partial \eta}\frac{\partial \theta}{\partial \eta}+Nt\left(\frac{\partial \theta}{\partial \eta}\right)^2-\frac{\partial \theta}{\partial \tau}=0 \tag{18}$$

$$\frac{\partial^2 \phi}{\partial \eta^2}+Le\,f\frac{\partial \phi}{\partial \eta}+\frac{Nt}{Nb}\frac{\partial^2 \theta}{\partial \eta^2}-\frac{\partial \phi}{\partial \tau}=0 \tag{19}$$

and are subjected to the boundary conditions

$$\begin{aligned} &f(0,\tau)=S,\quad \frac{\partial f}{\partial \eta}(0,\tau)=\lambda,\quad \theta(0,\tau)=1,\ \phi(0,\tau)=1\\ &\frac{\partial f}{\partial \eta}(\eta,\tau)\to A,\quad \theta(\eta,\tau)\to 0,\quad \phi(\eta,\tau)\to 0\quad \text{as}\quad \eta\to\infty \end{aligned} \tag{20}$$

To test the stability of the steady flow solution $f(\eta)=f_0(\eta)$, $\theta(\eta)=\theta_0(\eta)$ and $\phi(\eta)=\phi_0(\eta)$ satisfying the boundary-value problem (8)-(10), we write (see Weidman et al. [32] or Roşca and Pop [30]),

$$\begin{aligned} f(\eta,\tau)=f_0(\eta)+e^{-\gamma\tau}F(\eta,\tau),\ \theta(\eta,\tau)=\theta_0(\eta)+e^{-\gamma\tau}G(\eta,\tau),\\ \phi(\eta,\tau)=\phi_0(\eta)+e^{-\gamma\tau}H(\eta,\tau) \end{aligned} \tag{21}$$

where γ is an unknown eigenvalue parameter, and $F(\eta,\tau)$, $G(\eta,\tau)$ and $H(\eta,\tau)$ are small relative to $f_0(\eta)$, $\theta_0(\eta)$ and $\phi_0(\eta)$. Introducing (21) into Eqs. (17) - (19), we get the following linearized problem

$$\frac{\partial^3 F}{\partial \eta^3}+f_0\frac{\partial^2 F}{\partial \eta^2}+f_0''F-\left(2f_0'-\gamma\right)\frac{\partial F}{\partial \eta}+M\left(A-\frac{\partial F}{\partial \eta}\right)-\frac{\partial^2 F}{\partial \eta\,\partial \tau}=0 \tag{22}$$

$$\frac{1}{\Pr}\frac{\partial^2 G}{\partial \eta^2}+\left(f_0+Nb\phi_0'+2Nt\theta_0'\right)\frac{\partial G}{\partial \eta}+\theta_0'F+\gamma G+Nb\theta_0'\frac{\partial H}{\partial \eta}-\frac{\partial G}{\partial \tau}=0 \tag{23}$$

$$\frac{\partial^2 H}{\partial \eta^2}+Le\left(f_0\frac{\partial H}{\partial \eta}+\phi_0'F\right)+\frac{Nt}{Nb}\frac{\partial^2 G}{\partial \eta^2}+\gamma H-\frac{\partial H}{\partial \tau}=0 \tag{24}$$

along with the boundary conditions

$$\begin{aligned} &F(0,\tau)=0,\quad \frac{\partial F}{\partial \eta}(0,\tau)=0,\quad G(0,\tau)=0,\quad H(0,\tau)=0\\ &\frac{\partial F}{\partial \eta}(\eta,\tau)\to 0,\quad G(\eta,\tau)\to 0,\quad H(\eta,\tau)\to 0\quad \text{as}\quad \eta\to\infty \end{aligned} \tag{25}$$

The solution $f(\eta) = f_0(\eta)$, $\theta(\eta) = \theta_0(\eta)$ and $\phi(\eta) = \phi_0(\eta)$ of the steady equations (8) - (10) is obtained by setting $\tau = 0$. Hence $F = F_0(\eta)$, $G = G_0(\eta)$ and $H = H_0(\eta)$ in (22) - (24) identify initial growth or decay of the solution (21). In this respect, we have to solve the linear eigenvalue problem

$$F_0''' + f_0 F_0'' + f_0'' F_0 - \left(2f_0' - \gamma\right)F_0' + M\left(A - F_0'\right) = 0 \tag{26}$$

$$\frac{1}{\Pr} G_0'' + \left(f_0 + Nb\phi_0' + 2Nt\theta_0'\right)G_0' + \theta_0' F_0 + Nb\theta_0' H_0' + \gamma G_0 = 0 \tag{27}$$

$$H_0'' + Le\left(f_0 H_0' + \phi_0' F_0\right) + \frac{Nt}{Nb} G_0'' + \gamma H_0 = 0 \tag{28}$$

along with the boundary conditions

$$\begin{aligned} &F_0(0) = 0, \quad F_0'(0) = 0, \quad G_0(0) = 0, \quad H_0(0) = 0 \\ &F_0'(\eta) \to 0, \quad G_0(\eta) \to 0, \quad H_0(\eta) \to 0 \quad \text{as} \quad \eta \to \infty \end{aligned} \tag{29}$$

It should be stated that for particular values of $A, M, \Pr, Le, Nb, Nt$ and γ, the stability of the corresponding steady flow solution $f_0(\eta)$, $\theta_0(\eta)$ and $\phi_0(\eta)$ is determined by the smallest eigenvalue γ. As it has been suggested by Harris et al. [33], the range of possible eigenvalues can be determined by relaxing a boundary condition on $F_0(\eta)$ or $G_0(\eta)$. For the present problem, we relax the condition that $F_0'(\eta) \to 0$ as $\eta \to \infty$ and for a fixed value of γ we solve the system (26, 27,28) along with the new boundary condition $F_0''(0) = 1$.

Results and Discussions

The system of ordinary differential equations (8) – (10) subject to the boundary conditions (11) was solved numerically using the function bvp4c in MATLAB for different values of parameters: the stretching/shrinking parameter λ, suction parameter S, magnetic parameter M, velocity ratio parameter A, Brownian motion parameter Nb and thermophoresis parameter Nt. The Prandtl number Pr is set equal to 6.8 throughout the paper. The relative tolerance is set to 10^{-10}. The boundary conditions (11) at $\eta = \infty$ are replaced by $\eta = 10$. This choice is adequate for the velocity and temperature profiles to reach the far field boundary conditions asymptotically. We note that for $S = \lambda = M = 0$ and $A = 1$, the skin friction

coefficient ($f''(0) = 1.232587$) obtained is in excellent agreement with the result reported by Bejan [34] which gives rise to the confidence in the validity of our results.

In the present study, we intend to investigate the MHD stagnation point flow of a nanofluid over a stretching/shrinking sheet in the presence of suction effect at the boundary. The analysis shows that the existence of solution depends on the suction parameter S as well as the stretching/shrinking parameter λ as shown in the graph of the skin friction coefficient $f''(0)$ for different values of S against λ (Figure 2). From Figure 2, it is seen that for all values of S, unique solution exists for $\lambda > -2$ and $\lambda = \lambda_c$ where λ_c is the minimum values of λ for which the solution exist Furthermore, it is noted that the range of λ, where solutions exist, increases as S increases as seen in Table 1. This effect is compatible with the physics of the flow. The increasing suction at the sheet causes the generated vorticity to remain confined for greater value of magnitude of λ, with $\lambda \leq -2$, i.e. in case of larger shrinking rates than the stagnation flow rates and hence the range of existence of solution increases [35]. In addition, the range of solutions is also affected by the change in magnetic parameter M and velocity ratio parameter A. For future reference, we also include the values of λ_c for different values of M and A in Table 1.

The effect of suction, magnetic, velocity ratio and stretching/shrinking parameters on the skin friction coefficient are displayed in Figure 2 and Table 2. The skin friction coefficient decreases as λ increases. However, it increases with increasing S, M and A. From Figure 2, it is observed that the differences between the skin friction coefficient grow as the sheet keeps shrinking. From the lower branch, the skin friction coefficient is seen to approach 0 as λ approaches -2.

Figure 3 shows the effects of Brownian motion and thermophoresis parameter on the surface heat transfer rate (local Nusselt number). The local Nusselt number increases with λ. However, as Nb and Nt increase, the local Nusselt number decreases. This is due to the fact that the thermal boundary layer thickness will increase once Nb and Nt are intensified. This increment will lower the effectiveness of heat transfer capabilities of the fluid at the surface. It is interesting to note that the local Nusselt number for the three different values of Nb and Nt are shown to converge to approximately 0 at $\lambda = \lambda_c$. Furthermore, similar to Figure 2, from the lower branch, it is seen that the local Nusselt number approaches 0 as λ approaches -2.

Figs. 4 – 7 depict the samples of velocity and temperature profiles for different values of S, M, A and $Nt = Nb$. These profiles satisfy the far field boundary conditions (11) asymptotically, which support the validity of the results obtained, as well as supporting the

existence of dual solutions shown in Figs. 2 and 3. The velocity profiles in Figure 4 show that as suction increases, the velocity increases for upper branch and decreases for lower branch. Furthermore, it is observed that with the increasing suction, the boundary layer thickness decreases for the upper branch while it increases for the lower branch. This phenomenon concurs with Figure 2 (at λ = -2.4) where the skin friction coefficient increases for upper branch and decreases for lower branch as suction increases. Figs. 5 and 6 show the effects of magnetic parameter M and velocity ratio parameter A on the velocity for the shrinking sheet. However, at λ = -1, there is no lower branch in these figures as there is only unique solution for $\lambda > -2$. It is seen that for the increasing M and A, the velocity also increases. The profiles generated are qualitatively similar to those of Ibrahim et al. [31]. Also, the boundary layer thicknesses decrease as both M and A increase. In Figure 7, the temperature profiles generated show that the temperature increases as Nt and Nb increase. Furthermore, the profile supported the findings in Figure 3 where the boundary layer thickness increases as both Nt and Nb increase.

The numerical results show that dual solutions exist for Eqs. (8) – (10) with boundary conditions (11) when $\lambda \leq -2$. It is our intention to show that only the upper branch solutions are stable and physically realizable, while the lower branch solutions are not stable, and hence, not physically realizable. According to Weidman [32] and Merkin [36], as the eigenvalue γ = 0, Eqs. (26) – (28) yield the homogeneous problem which defines the critical value λ_c, which is the turning point value that separates the stable and unstable branches. The sign of γ will change at the turning point. Therefore, we solved the eigenvalue problem (26) – (28) to determine the smallest eigenvalues γ on the upper and lower solution branches. These results are displayed in Table 3 for several values of λ when S = 0.5 and $M = A$ = 1. The results show that positive values of γ are obtained at the upper branch while negative values of γ are found at the lower branch, confirming that the transitions from positive (stable) to negative (unstable) values of γ occur at the turning points of the parametric solution curves, which, as shown in Table 1, is λ_c = -2.4142. It is also noted that for both upper and lower branches, $|\gamma|$ decreases as λ approaches λ_c which confirms the observation of Merkin [36] where γ = 0 at $\lambda = \lambda_c$.

Conclusions

The magnetohydrodynamic (MHD) stagnation point flow of a nanofluid over a stretching/shrinking sheet with suction is studied. Numerical results were obtained using the

function bvp4c in MATLAB for several range of parameters: suction parameter, magnetic parameter, velocity ratio parameter, stretching/shrinking parameter, and Brownian motion and thermophoresis parameters. The results show that dual solutions exist. The range of the solution domain increases with increasing the suction effect at the boundary as well as the presence of magnetic field. Furthermore, increasing suction as well as the magnetic effect causes the skin friction coefficient to increase. Increasing the Brownian motion and thermophoresis parameters lower the local Nusselt number.

References

[1] Masuda H, Ebata A, Teramae K, Hishinuma N (1993) Alteration of thermal conductivity and viscosity of liquid by dispersing ultra-fine particles. Netsu. Bussei 7: 227-233.

[2] Choi SUS , Eastman JA (1995) Enhancing thermal conductivities of fluids with nanoparticles. in 1995 ASME International Mechanical Engineering Congress and Exposition. San Francisco, USA.

[3] Tiwari RK, Das MK (2007) Heat transfer augmentation in a two-sided lid-driven differentially heated square cavity utilizing nanofluids. International Journal of Heat and Mass Transfer 50: 2002-2018.

[4] Buongiorno J (2006) Convective transport in nanofluids. Journal of Heat Transfer 128: 240-250.

[5] Nield DA, Kuznetsov AV (2009) The Cheng–Minkowycz problem for natural convective boundary-layer flow in a porous medium saturated by a nanofluid. International Journal of Heat and Mass Transfer 52: 5792-5795.

[6] Nield DA, Kuznetsov AV (2009) Thermal instability in a porous medium layer saturated by a nanofluid. International Journal of Heat and Mass Transfer 52: 5796-5801.

[7] Nield DA, Kuznetsov AV (2011) The Cheng–Minkowycz problem for the double-diffusive natural convective boundary layer flow in a porous medium saturated by a nanofluid. International Journal of Heat and Mass Transfer 54: 374-378.

[8] Kuznetsov AV, Nield DA (2010) Natural convective boundary-layer flow of a nanofluid past a vertical plate. International Journal of Thermal Sciences 49: 243-247.

[9] Kuznetsov AV, Nield DA (2011) Double-diffusive natural convective boundary-layer flow of a nanofluid past a vertical plate. International Journal of Thermal Sciences 50: 712-717.

[10] Khan WA, Pop I (2010) Boundary-layer flow of a nanofluid past a stretching sheet. International Journal of Heat and Mass Transfer 53: 2477-2483.

[11] Bachok N, Ishak A, Pop I (2010) Boundary-layer flow of nanofluids over a moving surface in a flowing fluid. International Journal of Thermal Sciences 49: 1663-1668.

[12] Bachok N, Ishak A, Pop I (2012) Unsteady boundary-layer flow and heat transfer of a nanofluid over a permeable stretching/shrinnking sheet. International Journal of Heat and Mass Transfer 55: 2102-2109.

[13] Khan WA, Aziz A (2011) Natural convection flow of a nanofluid over a vertical plate with uniform surface heat flux. International Journal of Thermal Sciences 50: 1207-1214.

[14] Fischer EG (1976) Extrusion of Plastics, Wiley, New York.

[15] Wang CY (2002) Flow due to a stretching boundary with partial slip—an exact solution of the Navier–Stokes equations. Chemical Engineering Science 57: 3745-3747.

[16] Wang CY (2009) Analysis of viscous flow due to a stretching sheet with surface slip and suction. Nonlinear Analysis: Real World Applications 10: 375-380.

[17] Mandal IC, Mukhopadhyay S (2013) Heat transfer analysis for fluid flow over an exponentially stretching porous sheet with surface heat flux in porous medium. Ain Shams Engineering Journal 4: 103-110.

[18] Gupta PS, Gupta AS (1977) Heat and mass transfer on a stretching sheet with suction or blowing. The Canadian Journal of Chemical Engineering 55: 744-746.

[19] Andersson HI (2001) Slip flow past a stretching surface. Acta Mechanica 158: 121-125.

[20] Ishak A, Nazar R, Pop I (2009) Heat transfer over an unsteady stretching permeable surface with prescribed wall temperature. Nonlinear Analysis: Real World Applications 10: 2909-2913.

[21] Makinde OD, Aziz A (2011) Boundary layer flow of a nanofluid past a stretching sheet with a convective boundary condition. International Journal of Thermal Sciences 50: 1326-1332.

[22] Miklavčič M, Wang CY (2006) Viscous flow due to a shrinking sheet. Quarterly of Applied Mathematics 64: 283-290.

[23] Wang CY (2008) Stagnation flow towards a shrinking sheet. International Journal of Non-Linear Mechanics 43: 377-382.

[24] Fang T, Yao S, Zhang J, Aziz A (2010) Viscous flow over a shrinking sheet with a second order slip flow model. Communications in Nonlinear Science and Numerical Simulation 15: 1831-1842.

[25] Bachok N, Ishak A, Pop I (2011) Stagnation-point flow over a stretching/shrinking sheet in a nanofluid. Nanoscale Research Letters 6: Article ID 623 (10 pages).

[26] Bhattacharyya K, Mukhopadhyay S, Layek GC (2011) Slip effects on boundary layer stagnation-point flow and heat transfer towards a shrinking sheet. International Journal of Heat and Mass Transfer 54: 308-313.

[27] Lok YY, Ishak A, Pop I (2011) MHD stagnation point flow with suction towards a shrinking sheet. Sains Malaysiana 40: 1179–1186.

[28] Lok YY, Ishak A, Pop I (2011) MHD stagnation-point flow towards a shrinking sheet. International Journal of Numerical Methods for Heat & Fluid Flow 21: 61-72.

[29] Zaimi K, Ishak A, Pop I (2012) Boundary layer flow and heat transfer past a permeable shrinking sheet in a nanofluid with radiation effect. Advances in Mechanical Engineering 2012: Article ID 340354 (7 pages).

[30] Roşca AV, Pop I (2013) Flow and heat transfer over a vertical permeable stretching/shrinking sheet with a second order slip. International Journal of Heat and Mass Transfer 60: 355-364.

[31] Ibrahim W, Shankar B, Nandeppanavar MM (2013) MHD stagnation point flow and heat transfer due to nanofluid towards a stretching sheet. International Journal of Heat and Mass Transfer 56: 1-9.

[32] Weidman PD, Kubitschek DG, Davis AMJ (2006) The effect of transpiration on self-similar boundary layer flow over moving surfaces. International Journal of Engineering Science 44: 730-737.

[33] Harris SD, Ingham DB, Pop I (2009) Mixed convection boundary-layer flow near the stagnation point on a vertical surface in a porous medium: Brinkman model with slip. Transport in Porous Media 77: 267-285.

[34] Bejan A (2013) Convection Heat Transfer, John Wiley & Sons, New York.

[35] Bhattacharyya K, Layek GC (2011) Effects of suction/blowing on steady boundary layer stagnation-point flow and heat transfer towards a shrinking sheet with thermal radiation. International Journal of Heat and Mass Transfer 54: 302-307.

[36] Merkin JH (1985) On dual solutions occurring in mixed convection in a porous medium. Journal of Engineering Mathematics 20: 171-179.

Table 1 Values of λ_c

S	M	A	λ_c
0.5	1.0	1.0	-2.4142
1.0			-2.7755
2.0			-3.8116
0.5	0.1		-1.6088
	0.5		-1.9489
	1.0	1.5	-3.0827
		2.0	-3.7461

Table 2 Variation of the skin friction coefficient for different values of M and A when $S = 0.5$ and $\lambda = -1$

M	A	$f''(0)$
0.1	1.0	2.2195
0.5		2.6293
1.0		3.0516
0.1	1.5	3.7073
	2.0	5.2967

Table 3 The smallest eigenvalue γ when $S = 0.5$ and $M = A = 1$

λ	γ (Upper branch)	γ (lower branch)
-2.400	3.7393	-2.7709
-2.410	3.5737	-2.6594
-2.414	3.4331	-2.5509

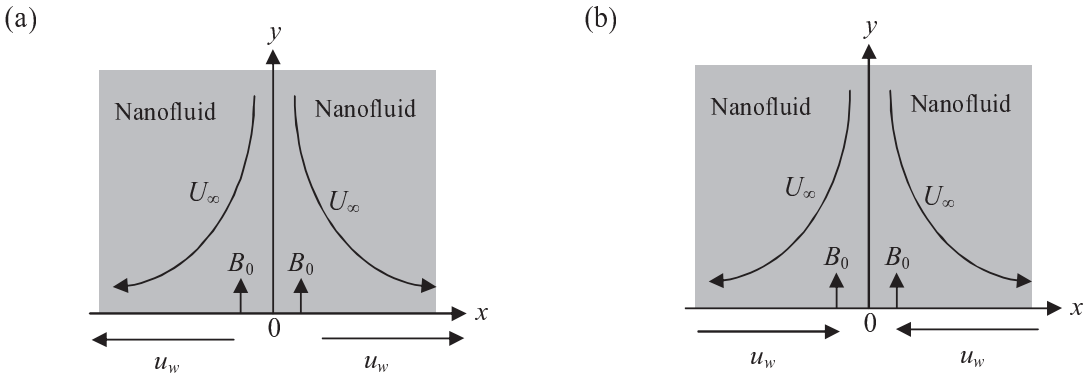

Fig 1. Geometry of the problem for (a) stretching sheet [29] and (b) shrinking sheet

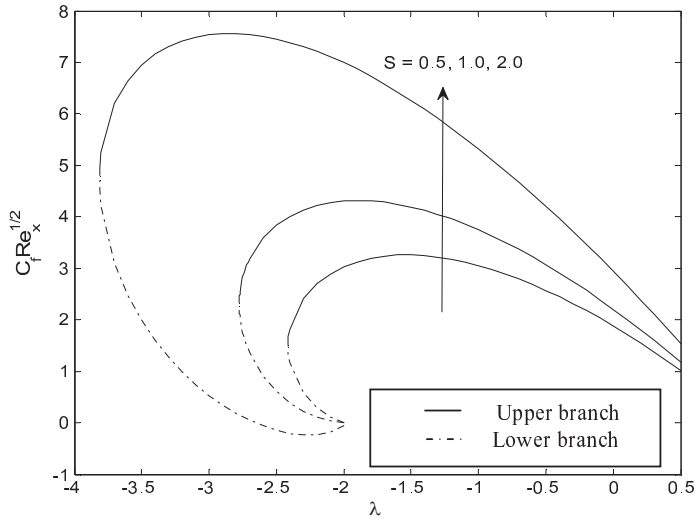

Fig. 2. Variation of the skin friction coefficient with λ for different values of S when $M = A = 1$

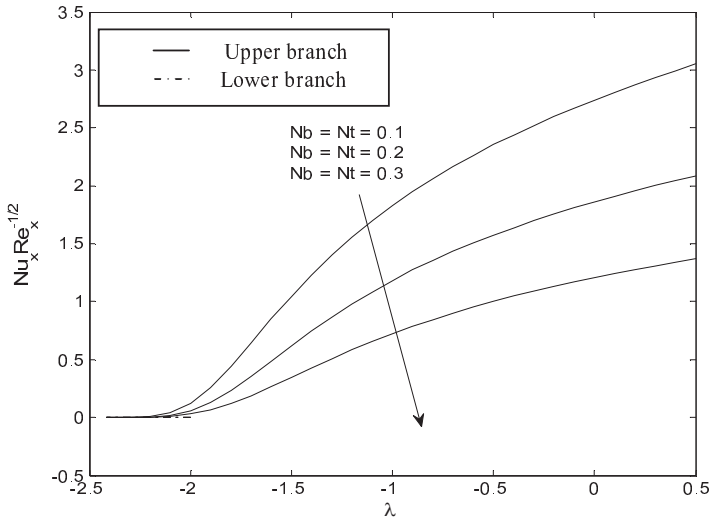

Fig. 3. Variation of the local Nusselt number with λ for different values of *Nb* and *Nt* when *S* = 0.5, *M* = *A* = 1, *Pr* = 6.8 and *Le* = 2

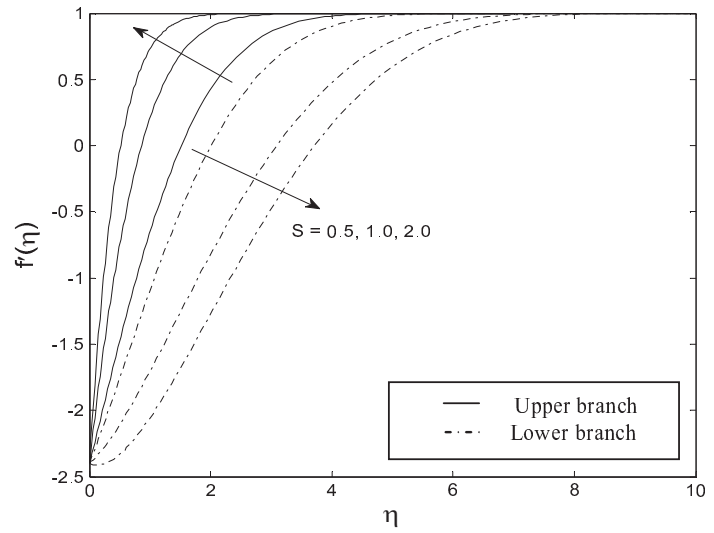

Fig. 4. The velocity profiles for different values of *S* when *M* = *A* =1 and λ = -2.4

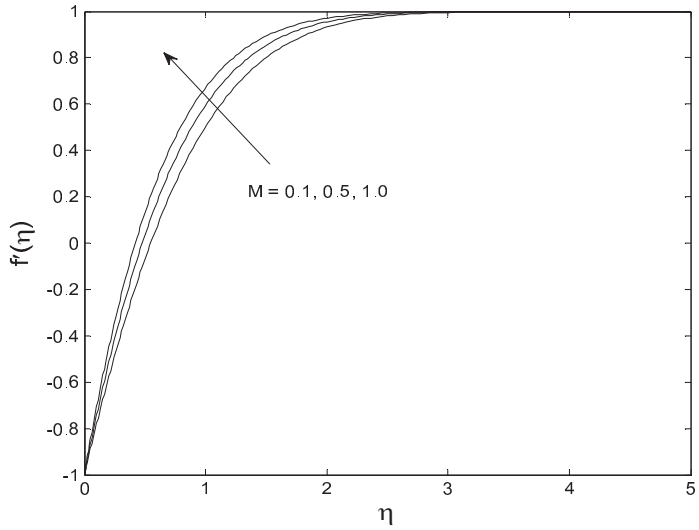

Fig. 5. The velocity profiles for different values of M when $S = 0.5$, $A = 1$ and $\lambda = -1$

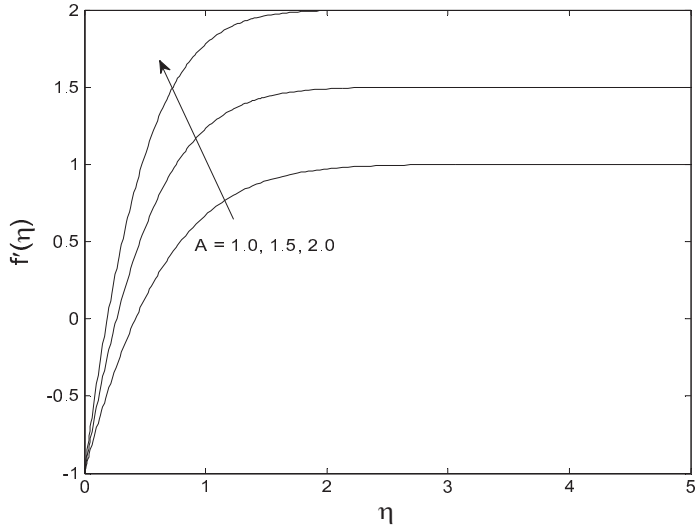

Fig. 6. The velocity profiles for different values of A when $S = 0.5$, $M = 1$ and $\lambda = -1$

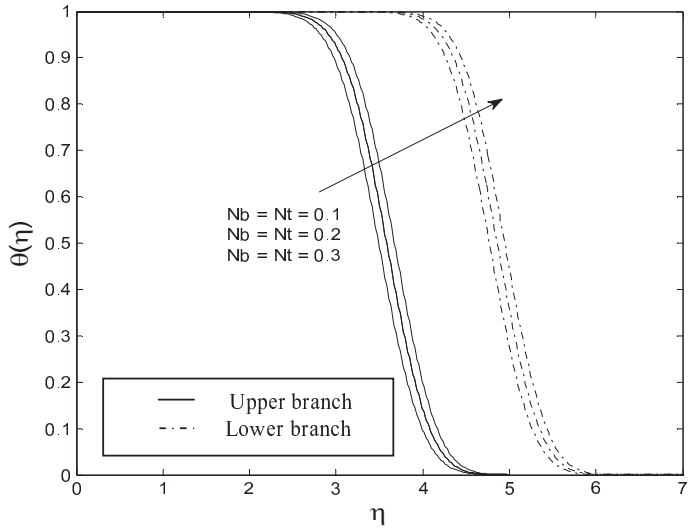

Fig. 7. The temperature profiles for different values of *Nb* and *Nt* when $S = 0.5$, $M = A = 1$, $Pr = 6.8$, $Le = 2$ and $\lambda = -2.4$